International Journal of Civil Engineering and Construction

E-ISSN: 2707-8337
P-ISSN: 2707-8329
Journal's Website
IJCEC 2025; 4(1): 20-35
Received: 10-01-2025
Accepted: 14-02-2025

Nouri Mahdi
Department of Civil Engineering, Akli Mohand Oulhadj University, Bouira, Algeria

Corresponding Author:
Nouri Mahdi
Department of Civil Engineering, Akli Mohand Oulhadj University, Bouira, Algeria

Parametric study of retaining wall stability under variable head loads using PLAXIS 2D

Nouri Mahdi

DOI: https://www.doi.org/10.22271/27078329.2025.v4.i1a.37

Abstract
Retaining walls are essential structures due to their cost and function, making their stability a critical concern, as failure from overturning or sliding can lead to significant damage. The design of these structures relies on various calculation methods, with numerical approaches providing greater accuracy in capturing soil behavior and the interaction between the wall and the ground. This study presents a bibliographical review of the principles and techniques used in the calculation of retaining walls, emphasizing the importance of precise modeling for ensuring their stability. The research focuses on the numerical modeling of a head-loaded reinforced concrete retaining wall to analyze the influence of key parameters on foundation bearing capacity and overall structural stability. A 5-meter-high wall with a 3.2-meter-wide base is modeled using PLAXIS 2D software, following a two-step approach: first, constructing the wall after excavating layers of sand and clay, and second, applying different load conditions of 10 kN/m², 100 kN/m², and 200 kN/m². The results provide valuable insights into the structural behavior of retaining walls under varying loads, contributing to improved design and safety practices.

Keywords: Retaining wall, load, foundation, bearing capacity, elastoplasticity, finite element, plaxis-V8 2D

Introduction

Retaining walls are, by definition, independent structures founded in order to contain the growth of the earth; in most cases, they are made to reduce the right-of-way caused by the embankments [1]. The calculation and the realization of retaining walls are more generally subject to the problems of the study and determination of the reactions of the soil on the wall [2]. The choice of the type of wall, its nature, and its dimensions are an almost direct consequence of the nature of the soil to be retained and its various physical and mechanical characteristics [3].

A retaining wall allows the containment of soil and must meet the following needs: avoid a landslide caused either by a dynamic or static load (e.g., a building above the surface) or hold a surface so that it is not sliding on a building adjacent to the surface [4].

The purpose of this thesis is to study the stability of a retaining wall subjected to head loading. To achieve our objective, we began a bibliographical study on retaining structures, the calculation of the pressures of the grounds, as well as numerical modeling [5]. This research is part of the study of modeling the behavior of retaining walls by certain parameters related to the mechanism of rupture [6].

Description of the Project

Presentation of the Case Study

The studied case consists in analyzing the behavior of a reinforced concrete retaining wall with a height of 6 m and a width of 0.4 m (thickness). The soil profile consists of a 2 m layer of sand resting on a layer of clay; the characteristics of each parameter are listed in Table 1 [7]. The excavation consisted of digging 2 m of sand followed by 3 m of clay. Then, the backfill of 20 m wide was ensured by a retaining wall with anchoring abutments. At the end, we proposed cases and activation of loads (Forces applied) on the wall: 10 kN/m², 100 kN/m², and 200 kN/m² [10]. The behavior of retaining structures made of blocks with soil infill has been modeled using advanced numerical techniques [24].

The workflow of the two phases is illustrated in Figure 1, which depicts the geometry of the model. The successful completion of the phases, including the application of loads, is shown in Figure 4.

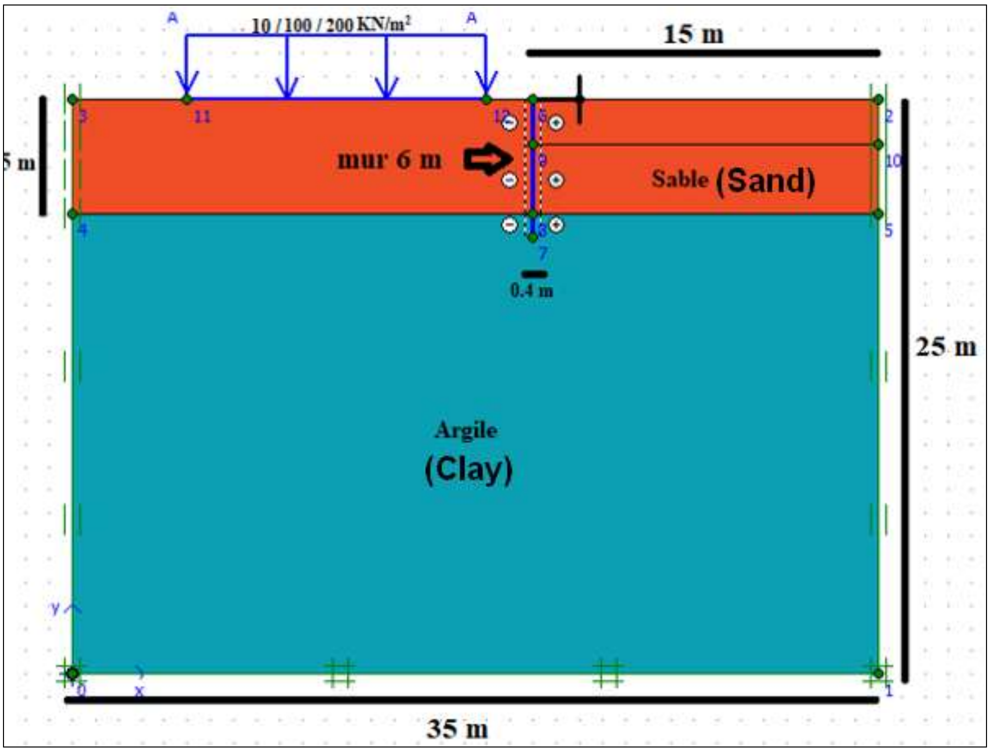

Fig 1: Geometry of the model.

Geotechnical Data

Numerical modeling by the PLAXIS calculation code, like any other code, requires the definition of some parameters. The soil parameters and the characteristics of the retaining wall are summarized in Table 1. The structural properties of the retaining wall and anchor bolts are detailed in Table 2 and Table 3, respectively [8].

Table 1: Geotechnical Properties of Sand and Clay.

Material characteristics	Clay	Sand
Behavioral model	Mohr coulomb	Mohr coulomb
Type	Drained	Drained
Young'smodulus E (Kpa)	20000	13000
Poisson coefficient ν	0.350	0.30
Dry density γ (KN/m^3)	16	17
Saturateddensity γsat (KN/m^3)	18	20
Friction angle φ' (°)	25	31
Angle of dilatancyψ (°)	0	1
Cohesion C'(Kpa)	10	1
Horizontal permeabilitykx (m / day)	0.001	1
Vertical permeabilityky (m / day)	0.001	1
1) Interface reduction factor R_{inter}	2) 1	3) 1

Table 1 summarizes the soil parameters, listing key characteristics such as Young's modulus, Poisson's ratio, and density.

Explanation: These parameters were obtained from literature sources [12, 14, 19] and PLAXIS input data.

Justification: The use of Rinter = 1 assumes full shear strength at the interface, which is uncommon in practical geotechnical engineering. A discussion on this assumption is recommended.

The behavioral model used to simulate the embank mentis the line are lastic, perfectly plastic model with the Mohr-Coulomb plasticity criterion included in the PLAXIS code.

Table 2. Retaining Wall Structural Properties.

Parameter	Wall
Type of behavior	Lineare lastic
Normal stiffness EA (KN/m)	4×10^6
Flexur alrigidity EI (KN. m^2/m)	3.5×10^6
The weight W (KN/m/m)	20
Poisson coefficient ν	0.35
Equivalent thickness d (m)	3,240
A	11.8
4) B	5) 6.35×10^{-6}

Table 3: Anchor bolt characteristics [19].

Parameter	Anchor bolts
Type of behavior	Elastic
Normal stiffnessA (KN/m)	6) 2×10^5

Explanation: These values were sourced from engineering design standards and PLAXIS input data.

Contribution to reducing displacement and stress is not analyzed in the results section. Further numerical analysis is recommended.

The study assumes Rinter = 1, which implies full shear strength transfer at the soil-wall interface. However, real-world conditions often result in Rinter values between 0.7 and 0.8 due to partial slippage at the interface.

Geotechnical Properties

Choice of Mohr-Coulomb Parameters

The Mohr-Coulomb (MC) model was selected for its simplicity and widespread use in geotechnical engineering. It is a linear elastic-perfectly plastic model that assumes a linear relationship between shear stress and normal stress, defined by the cohesion (C') and the angle of internal friction (φ'). This model is particularly suitable for soils that exhibit a clear failure criterion, such as sand and clay, which are the primary materials in this study. The MC model is also computationally efficient, making it a practical choice for preliminary analyses.

Justification for Rinter = 1

The interface reduction factor (Rinter) is set to 1, which implies full shear strength transfer at the soil-wall interface. This assumption is made to simplify the initial analysis and to avoid the complexities associated with partial slippage at the interface. However, in real-world scenarios, Rinter typically ranges between 0.7 and 0.8 due to partial slippage and imperfect contact between the soil and the wall. The assumption of Rinter = 1 may overestimate the shear strength at the interface, leading to potentially conservative results. Future studies should consider varying Rinter to assess its impact on the wall's stability and displacement.

Modeling and calculation

Finite Element Modeling (FEM) Details.

Mesh Setup

The study does not specify whether a structured or unstructured mesh was used in PLAXIS 2D. The mesh density and refinement method significantly influence the accuracy of numerical simulations. A structured mesh, with uniform element distribution, is often used for simpler geometries, while an unstructured mesh can better handle complex geometries and localized refinements. For future studies, it would be beneficial to specify the type of mesh used (e.g., triangular or quadrilateral elements) and conduct a sensitivity analysis on mesh size and refinement to ensure that the results are independent of meshing artifacts [9].

Future studies could explore large deformation analysis using advanced finite element methods [23].

Boundary Conditions

The study does not detail the boundary conditions applied to the model. Boundary conditions are crucial for ensuring that the model behaves realistically. Typically, in geotechnical simulations, the lateral boundaries are assigned roller supports (restricting only horizontal displacement) to simulate the natural confinement of the soil, while the bottom boundary is fixed (restricting both vertical and horizontal movement). The lateral boundary distance should be sufficient to prevent artificial constraints on soil deformation. Clarifying the boundary conditions used in the study would improve the transparency and reliability of the results [10].

Load Application

The study applies head loads of 10, 100, and 200 kN/m² but does not provide a clear justification for these specific values [11]. These loads could represent various real-world scenarios:

1. **10 kN/m²:** This load might represent light construction equipment or minor traffic loads.
2. **100 kN/m²:** This load could correspond to heavier construction equipment, such as cranes or trucks, or significant traffic loads.
3. **200 kN/m²:** This load might represent extreme conditions, such as heavy machinery or seismic pressures.

The response of retaining walls under dynamic loads has been extensively studied using numerical methods [22].

Comparing these loads with typical real-world surcharge values in geotechnical engineering would provide better context for the study. For example, traffic loads on highways typically range from 10 to 20 kN/m², while construction loads can vary significantly depending on the equipment used. The selection of these loads should be justified based on realistic scenarios that the retaining wall might encounter during its service life.

Comparison with Realistic Construction or Traffic Loads

In practical geotechnical engineering, retaining walls are often subjected to surcharge loads from construction activities, traffic, or adjacent structures. For example:

Traffic Loads: Highway traffic loads are typically in the range of 10-20 kN/m², while heavy truck loads can reach up to 50 kN/m².

Construction Loads: Construction equipment such as cranes or bulldozers can impose loads ranging from 50 to 200 kN/m², depending on the equipment's weight and distribution.

Seismic Loads: In seismic zones, retaining walls may be subjected to dynamic loads that can significantly exceed static loads, depending on the earthquake's magnitude and the soil's response.

The chosen load values (10, 100, and 200 kN/m²) should be compared with these typical values to ensure that the study covers a realistic range of loading conditions. This comparison would help validate the relevance of the study's findings to real-world applications.

Soil Behavior Model Selection

The study employs the Mohr-Coulomb (MC) model but does not explain why alternative soil behavior models were not considered [12]. The Mohr-Coulomb model assumes elastic-perfectly plastic behavior, with no consideration of stress-dependent stiffness or strain-hardening/softening behavior. While this model was chosen for its simplicity, future studies could explore more advanced models such as the Hardening Soil Model (HSM), which captures stress-dependent stiffness and provides more realistic predictions for medium to highly compacted soils. A comparative analysis with the Hardening Soil Model could determine its influence on the results.

Advanced soil models, such as the anisotropic bounding surface model, have been shown to improve the accuracy of simulations in clays [16].

The calculation of the stability of the retaining wall with Plaxis consists of using the following construction procedure:

1. Installation of retaining wall with anchorage to support the wall following the addition of an initial load (example: 10 KN/m^2 with a distance of 2 m behind the wall) [18].
2. Excavation 1: remove a layer of sand approximately 2 meters.
3. Excavation 2 + construction: remove a 3 meter layer of sand and then build a retaining wall.
4. Addition of a new load 100 KN/m2 at a distance of 2 m behind the wall [17].
5. Addition of a new load 200 KN/m2 at a distance of 2 m behind the wall [15].

The initial part of the project will be presented in the initial phase [15].

Figure 2 represents the initial phase of retaining wall installation, while Figure 3 illustrates the addition of initial loads of 10, 100, and 200 KN/m².

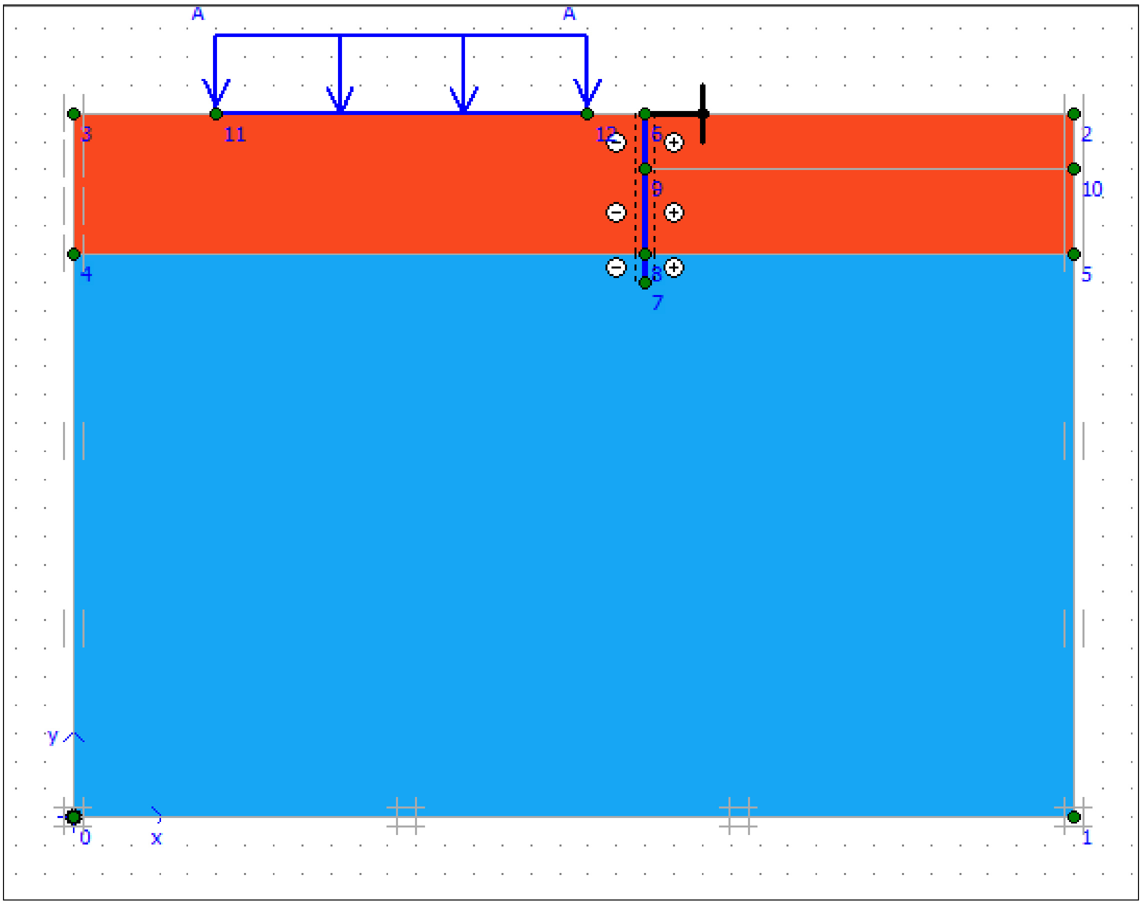

Fig 2: Initial phase representation with Plaxis and retaining wall installation with an anchor.

Installation of a retaining wall with an anchor to support the wall following the addition of an initial load (example: 10 KN/m^2, 100 KN/m^2, 200 KN/m^2) [11].

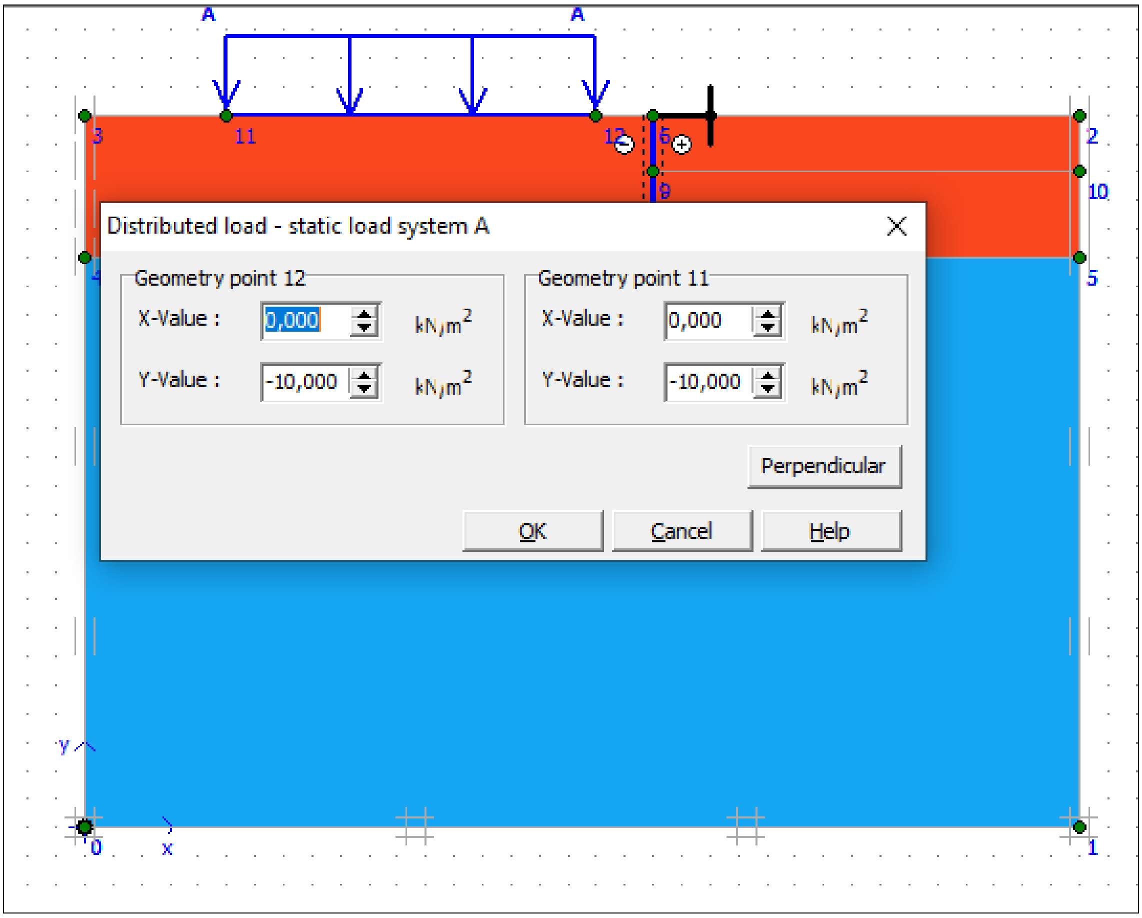
Distributed load - static load system A
Geometry point 12
X-Value : 0,000 kN/m2
Y-Value : -10,000 kN/m2
Geometry point 11
X-Value : 0,000 kN/m2
Y-Value : -10,000 kN/m2
Perpendicular
OK
Cancel
Help

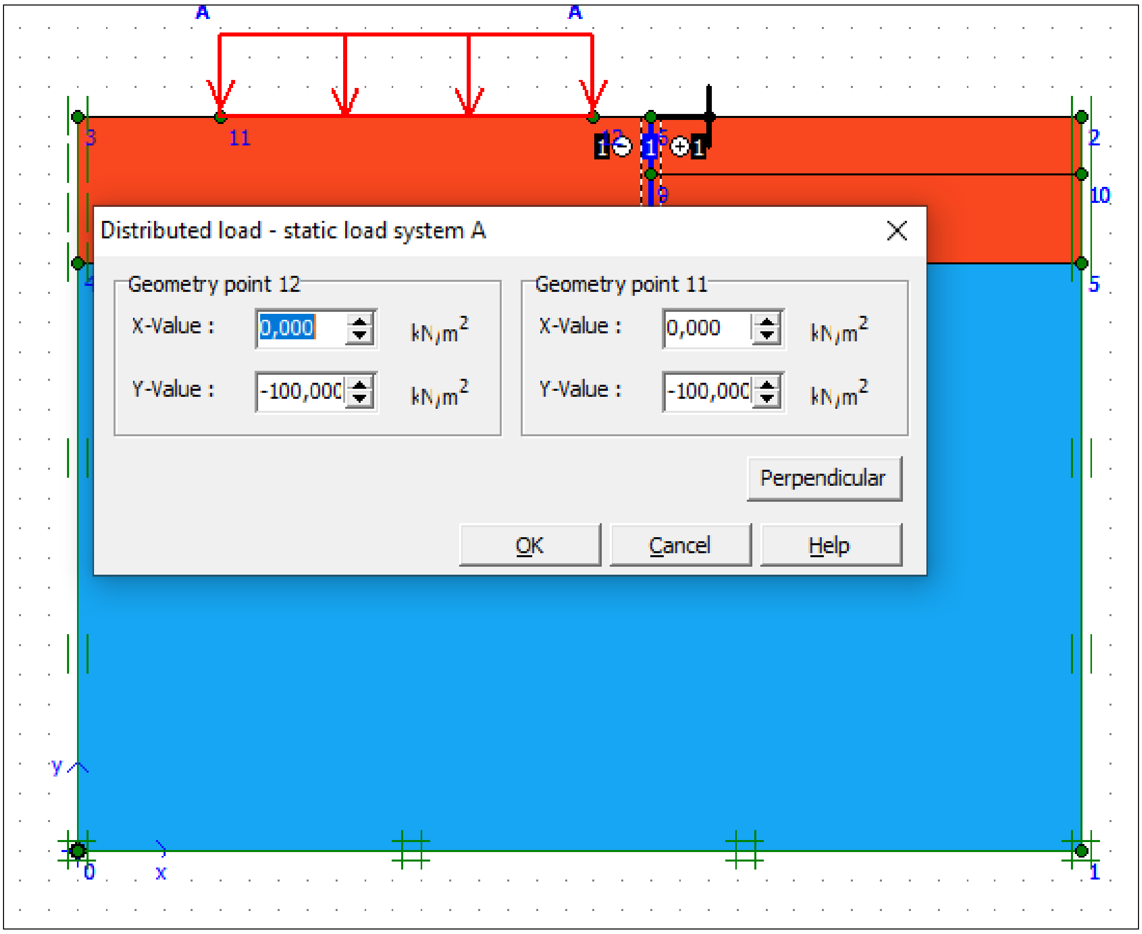
Distributed load - static load system A
Geometry point 12
X-Value : 0,000 kN/m2
Y-Value : -100,000 kN/m2
Geometry point 11
X-Value : 0,000 kN/m2
Y-Value : -100,000 kN/m2
Perpendicular
OK
Cancel
Help

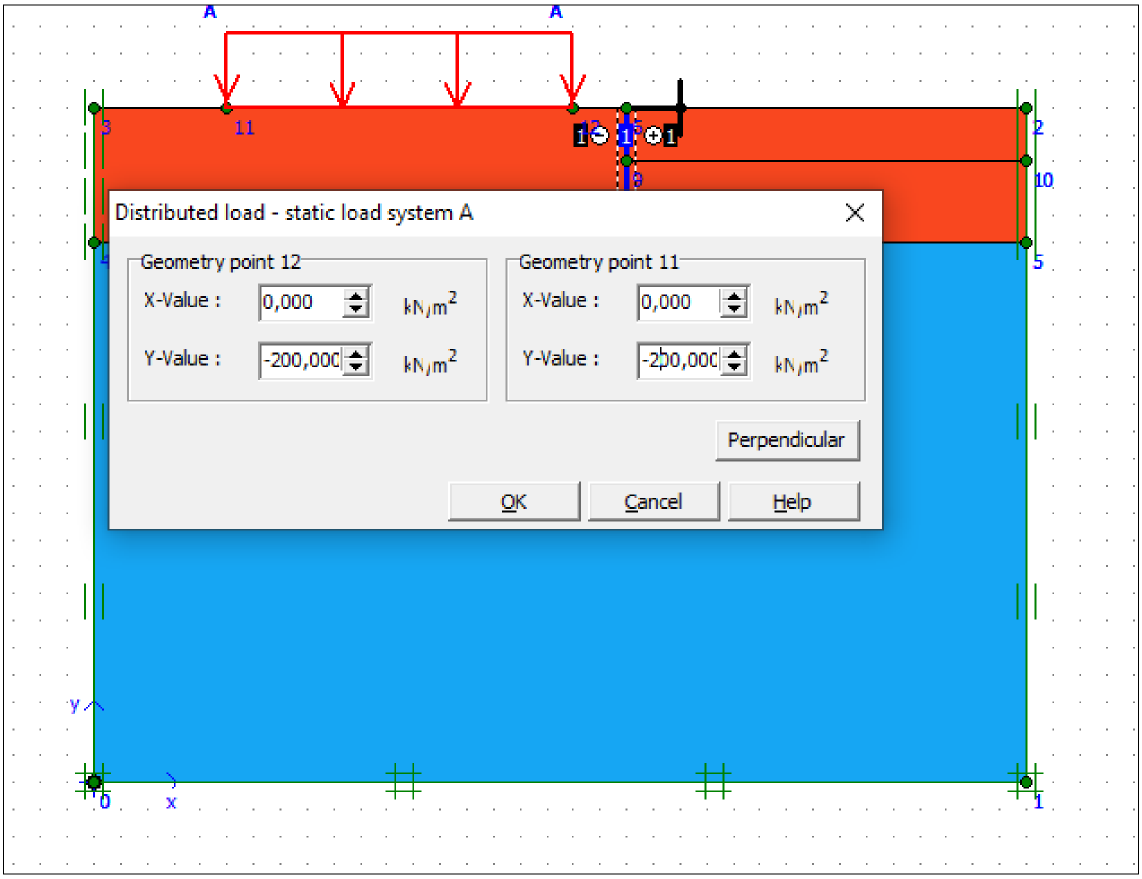

Fig 3(a): Application of 10 KN/m² load, (b): Application of 100 KN/m² load, (c): Application of 200 KN/m² load. [20].

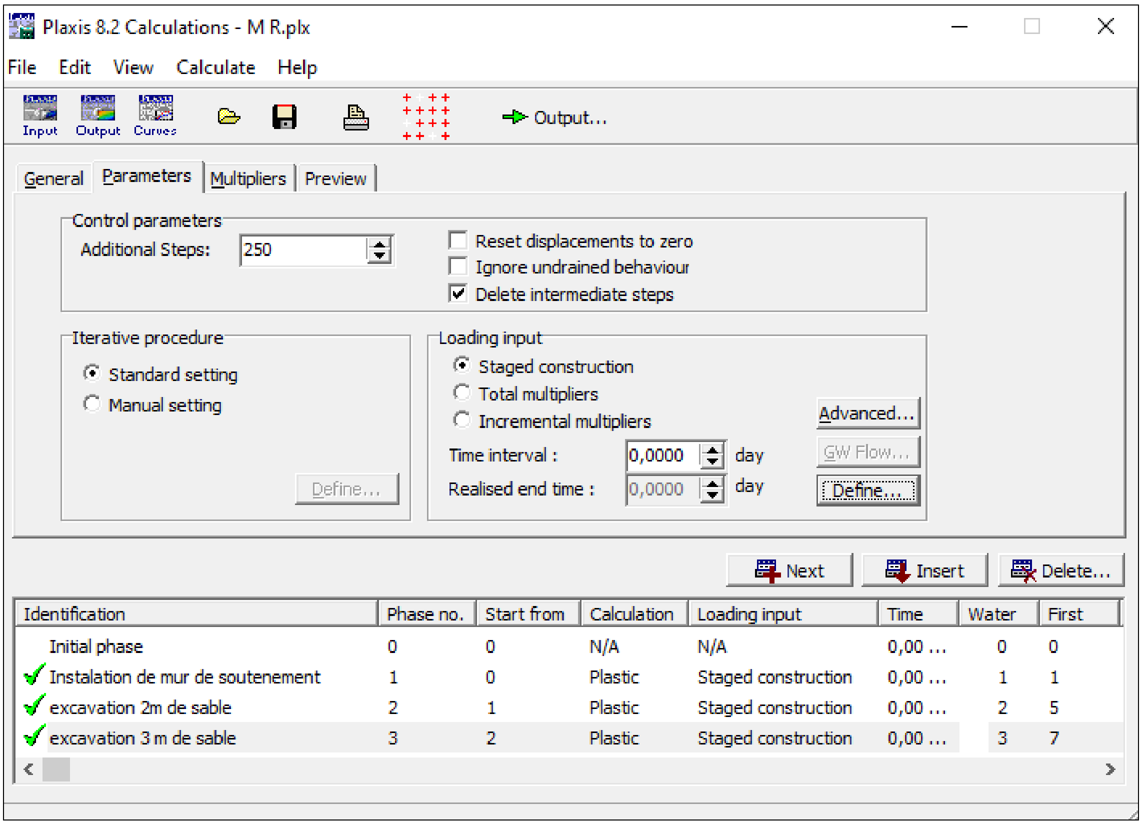

Fig 4: Representation of the successful completion of the phases with Plaxis [20].

Representation of the results obtained in the form of diagrams of curves:

Figures 5 through 7 present the deformation of the mesh, total displacement, and total stress distributions, respectively.

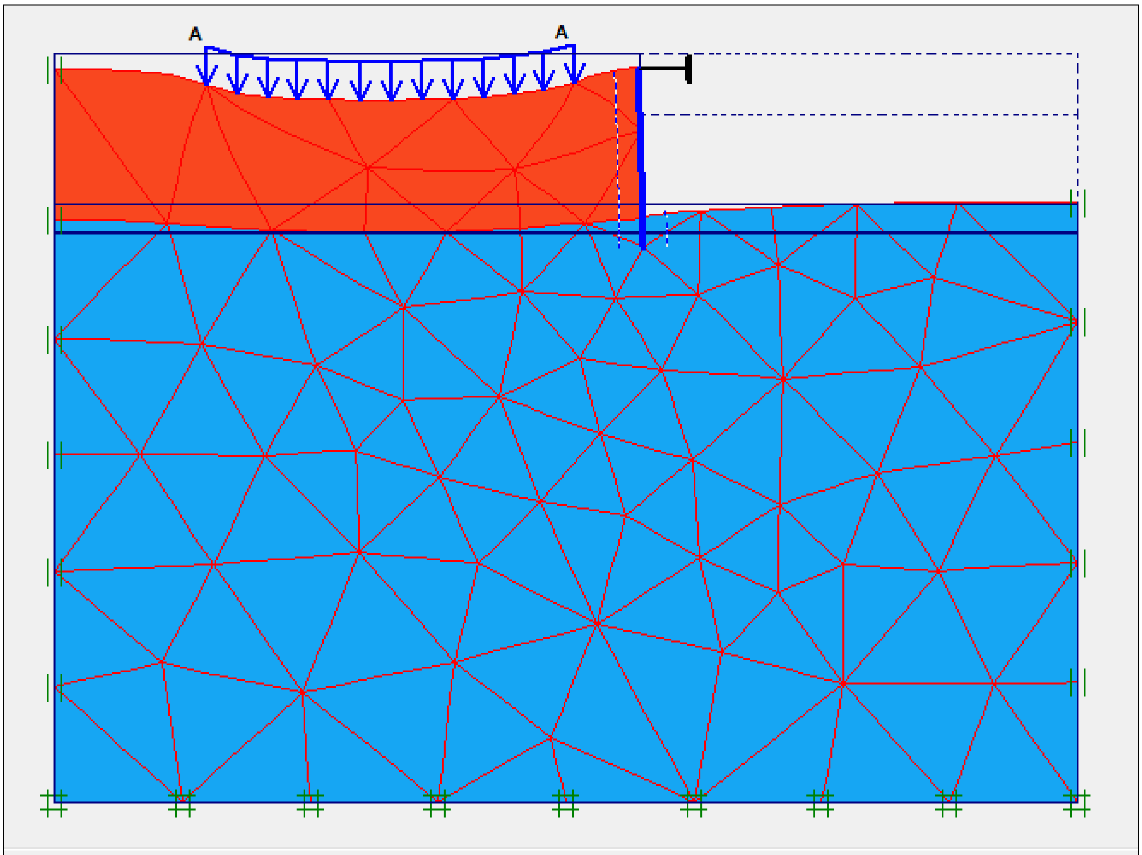

Deformed Mesh
Extreme total displacement 7,67*10 $^{-3}$ m
(displacements scaled up 200,00 times)

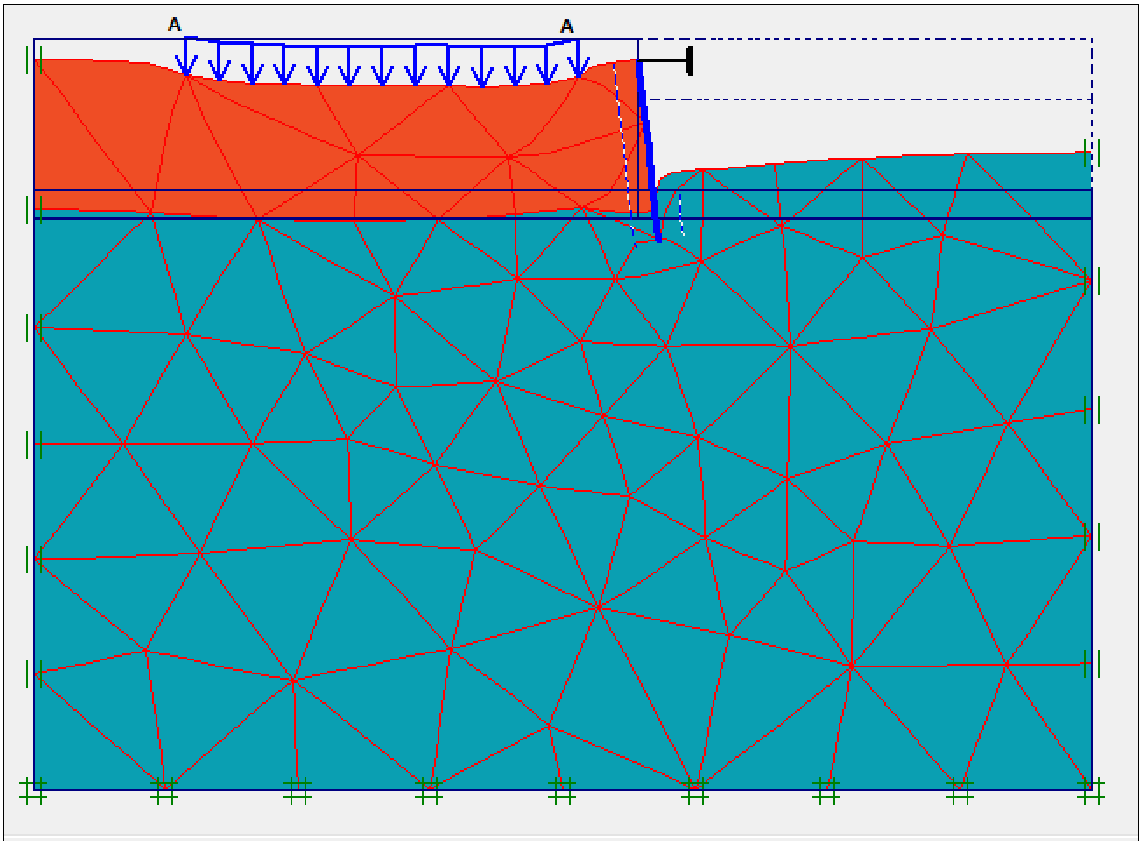

Deformed Mesh
Extreme total displacement 79,81*10 $^{-3}$ m
(displacements scaled up 20,00 times)

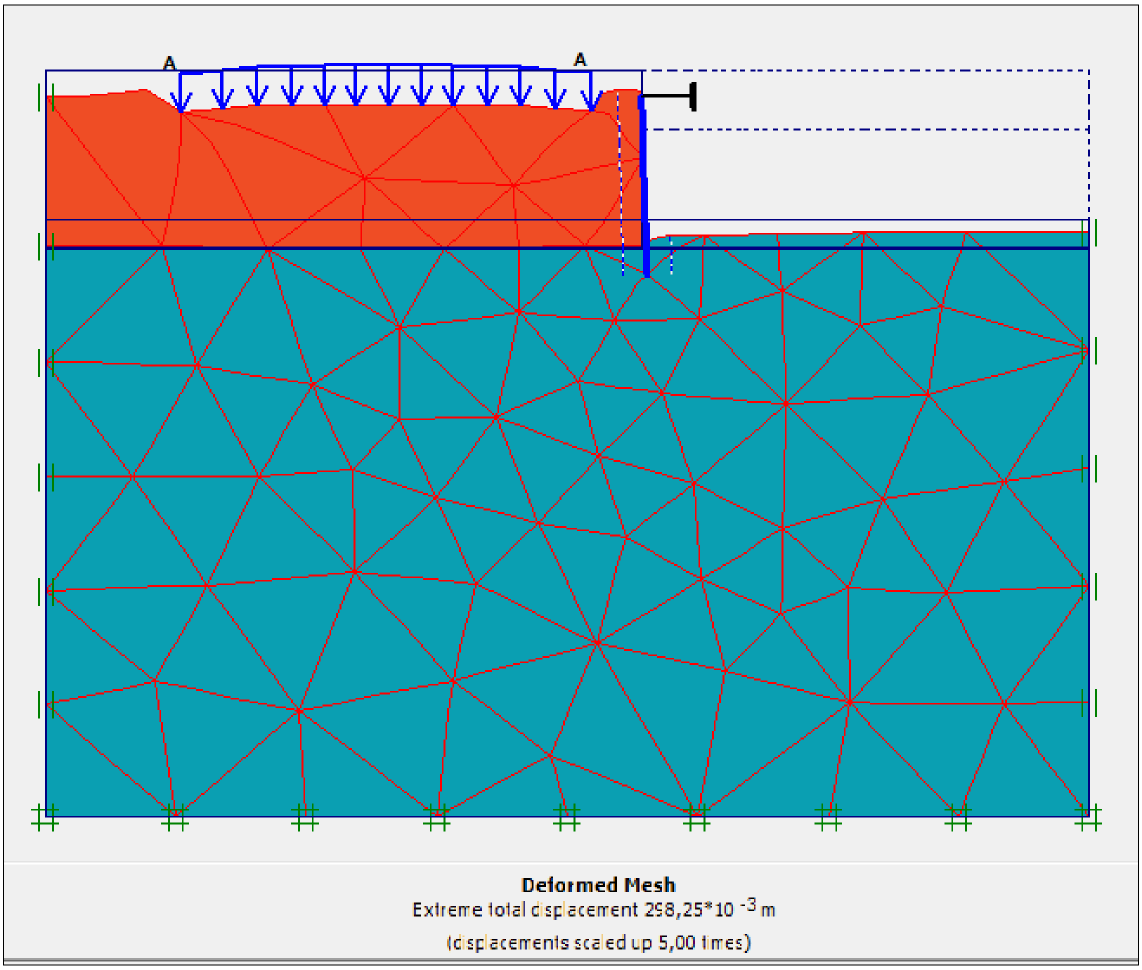

Fig 5(a): Mesh deformation for 10 KN/m² load, (b): Mesh deformation for 100 KN/m² load, (c): Mesh deformation for 200 KN/m² load.

X-axis: Distance along the retaining wall (m)
Y-axis: Vertical displacement (mm)
Legend:
Blue line: 10 kN/m² load
Note: The red and green lines (representing 100 kN/m² and 200 kN/m² loads) are not visible in the figure.

The mesh deformation (Figure 5) shows that higher loads lead to increased displacement, particularly in the upper portion of the wall, indicating potential plastic deformation in the soil.

Description: Figures 6 and 7 illustrates the deformation patterns of the mesh under different head load conditions. As the load increases, displacement increases, particularly in the upper portion of the wall.

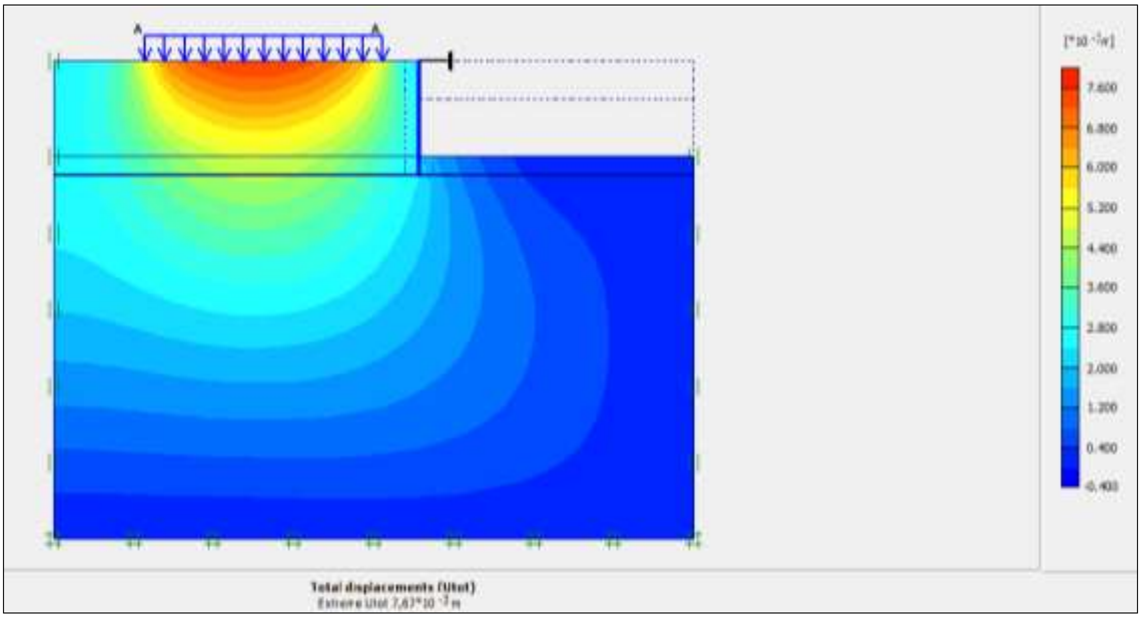

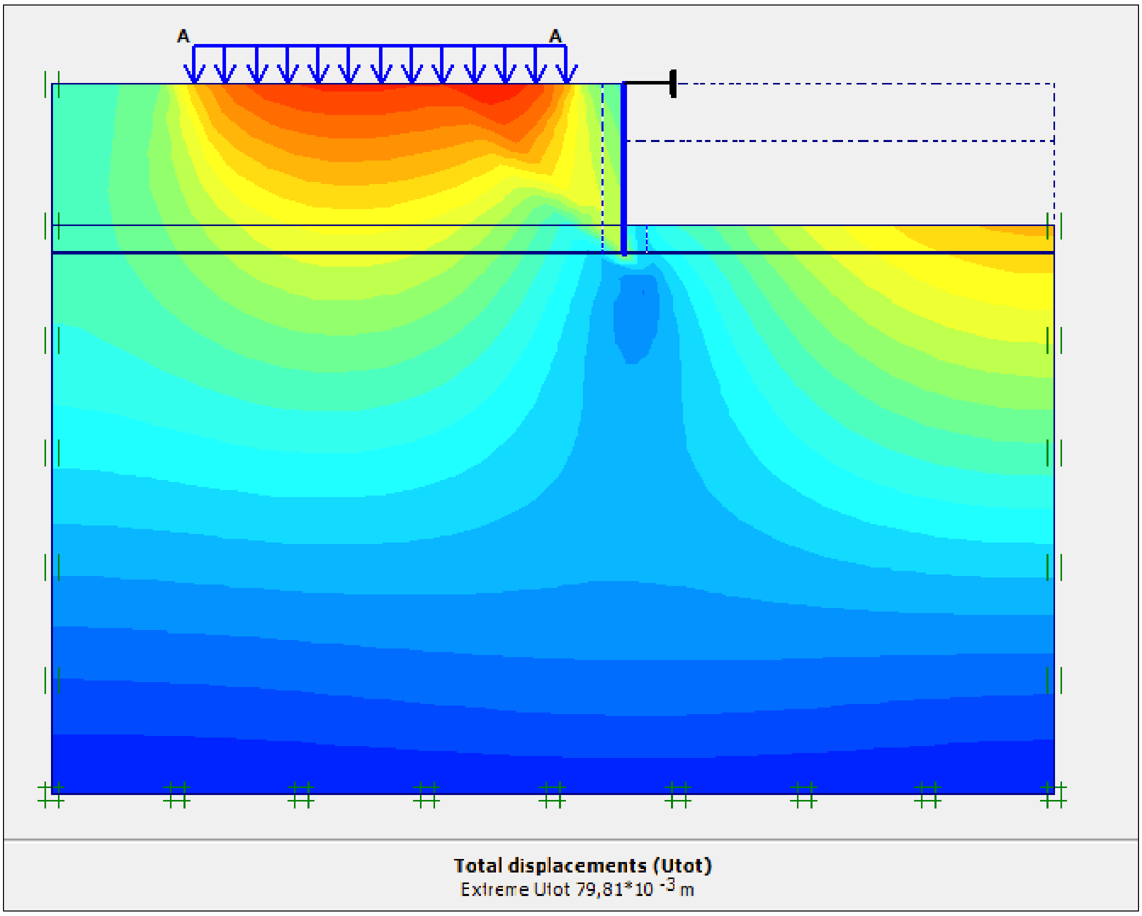

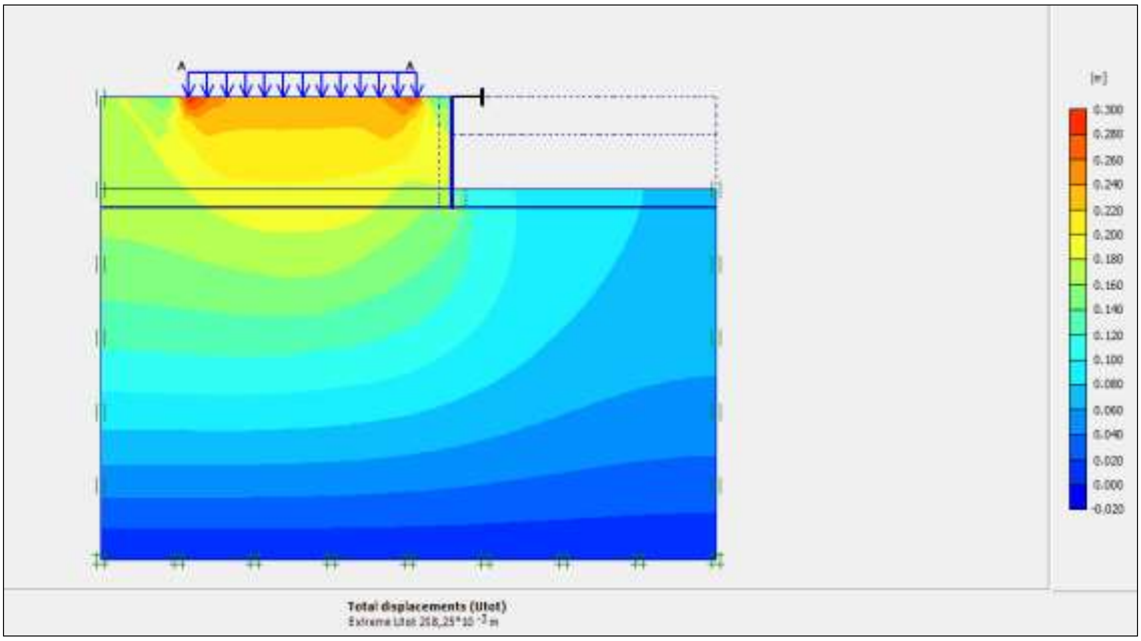

Fig 6(a): Total displacement for 10 KN/m², (b): Total displacement for 100 KN/m², (c): Total displacement for 200 KN/m².

X-axis: Distance along the wall (m)
Y-axis: Total displacement (mm)
Legend:
Blue line: 10 kN/m² load
Note: The red and green lines (representing 100 kN/m² and 200 kN/m² loads) are not visible in the figure.

Description: Figure 6 (a), (b), (c) compares the total displacement observed at different points along the retaining wall for each loading condition. At 200 kN/m², the structure exhibits significant displacement, suggesting plastic deformation in the soil.

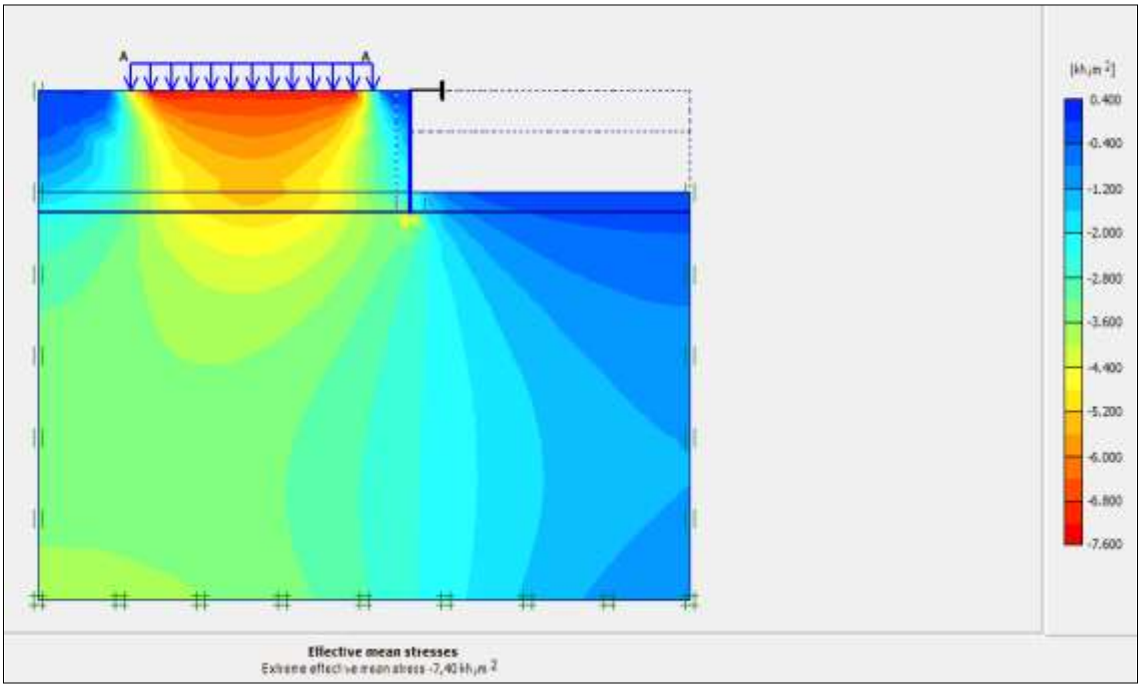
A
A
[kN/m²]
0.400
-0.400
-1.200
-2.000
-2.800
-3.600
-4.400
-5.200
-6.000
-6.800
-7.600
Effective mean stresses
Extreme effective mean stress -7,40 kN/m²

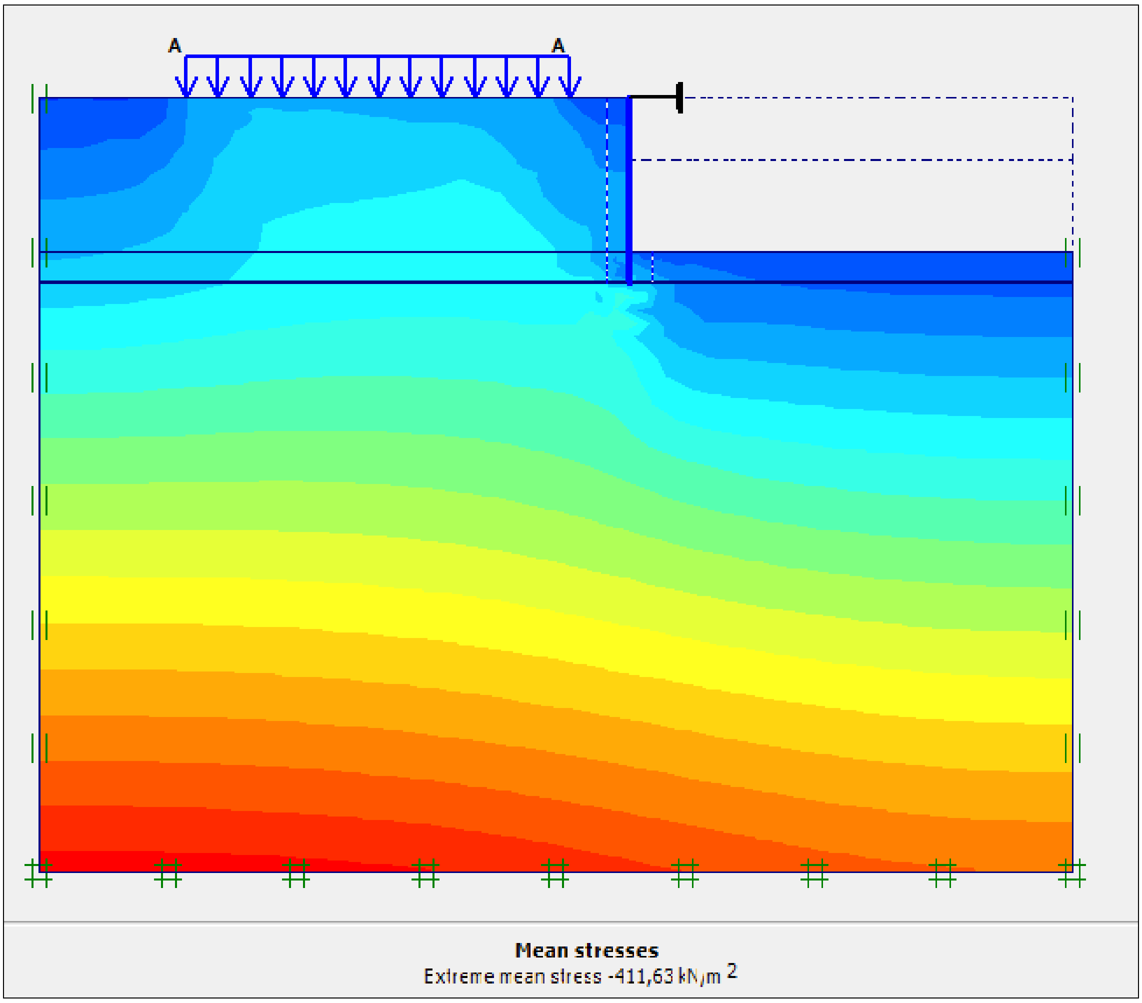
A
A
Mean stresses
Extreme mean stress -411,63 kN/m²

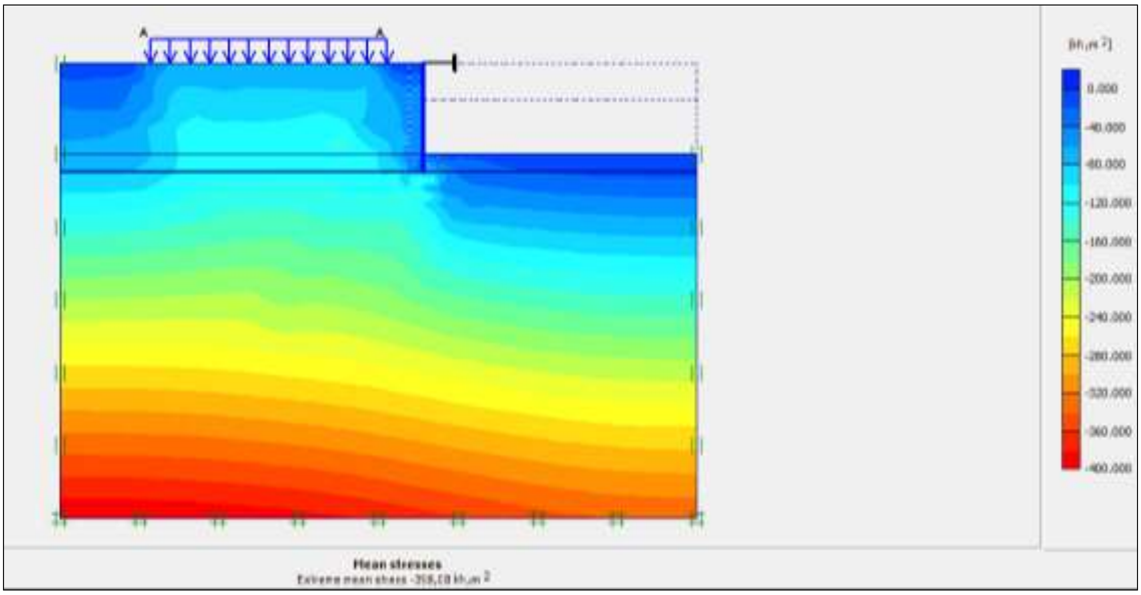

Fig 7(a): Total stress for 10 KN/m², (b): Total stress for 100 KN/m², (c): Total stress for 200 KN/m².

X-axis: Distance along the retaining wall (m)
Y-axis: Stress (kPa)
Legend:
Blue line: 10 kN/m² load
Note: The red and green lines (representing 100 kN/m² and 200 kN/m² loads) are not visible in the figure.
Description: The stress distribution along the retaining wall is shown for different applied loads. The stress concentration increases significantly at 200 kN/m², indicating the onset of plasticity in the soil medium.

The choice of the points (a random selection)

1) To have the displacement graphs we have chosen the following points: A, B, C, D behind the wall.
2) To have the graphs of the constraints we have chosen the following points: E, F, J, H behind the wall.

Represent on the following figure (08)

The selected points for displacement and stress analysis are depicted in Figure 8.

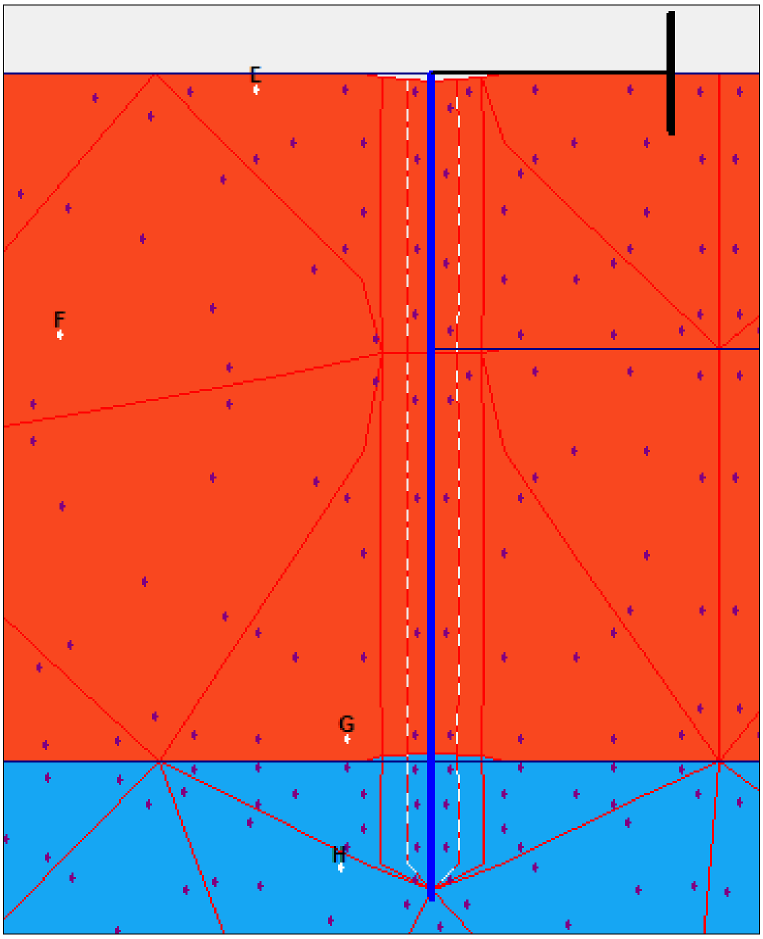

Fig 8(a): Layout of selected displacement points, (b): Layout of selected stress points.

Displacement graphs

The variation of displacement and stress across the three cases studied is detailed in Figures 9 through 11.

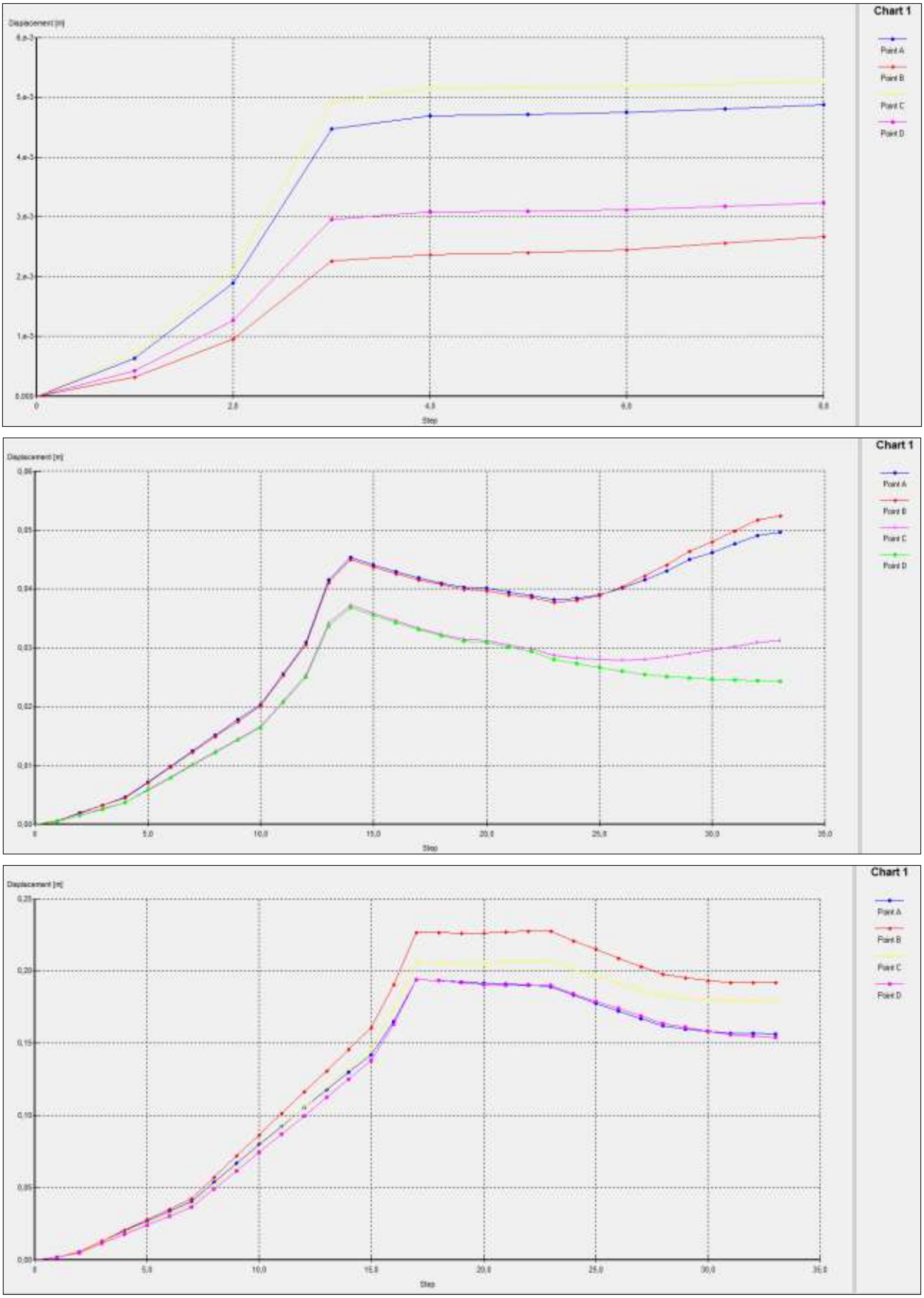

Fig 9(a): Total displacement curve for 10 KN/m², (b): Total displacement curve for 100 KN/m², (c): Total displacement curve for 200 KN/m².

Constraint graphs

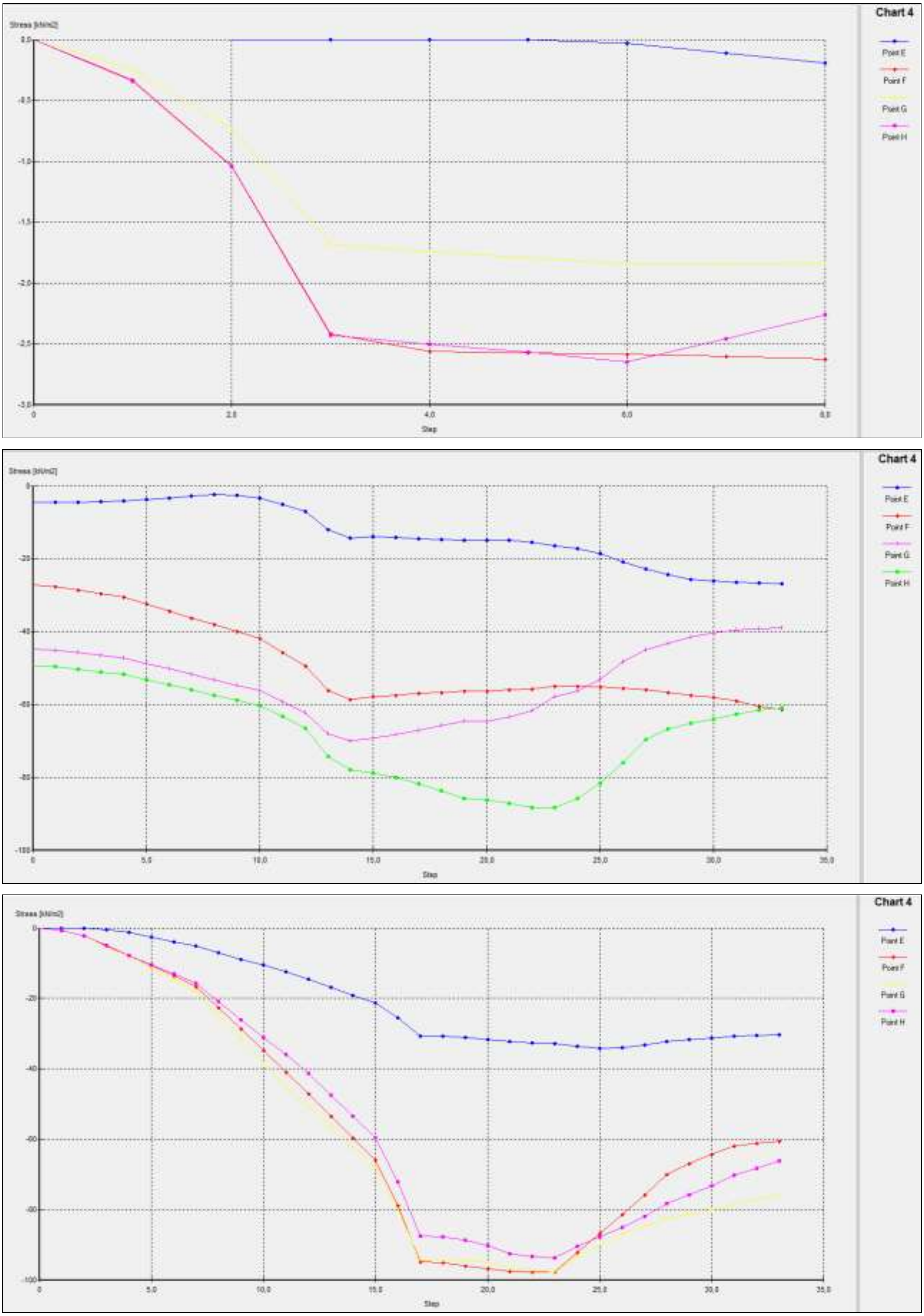

Fig 10(a): Stress distribution along xx' for 10 KN/m², (b): Stress distribution along xx' for 100 KN/m², (c): Stress distribution along xx' for 200 KN/m².

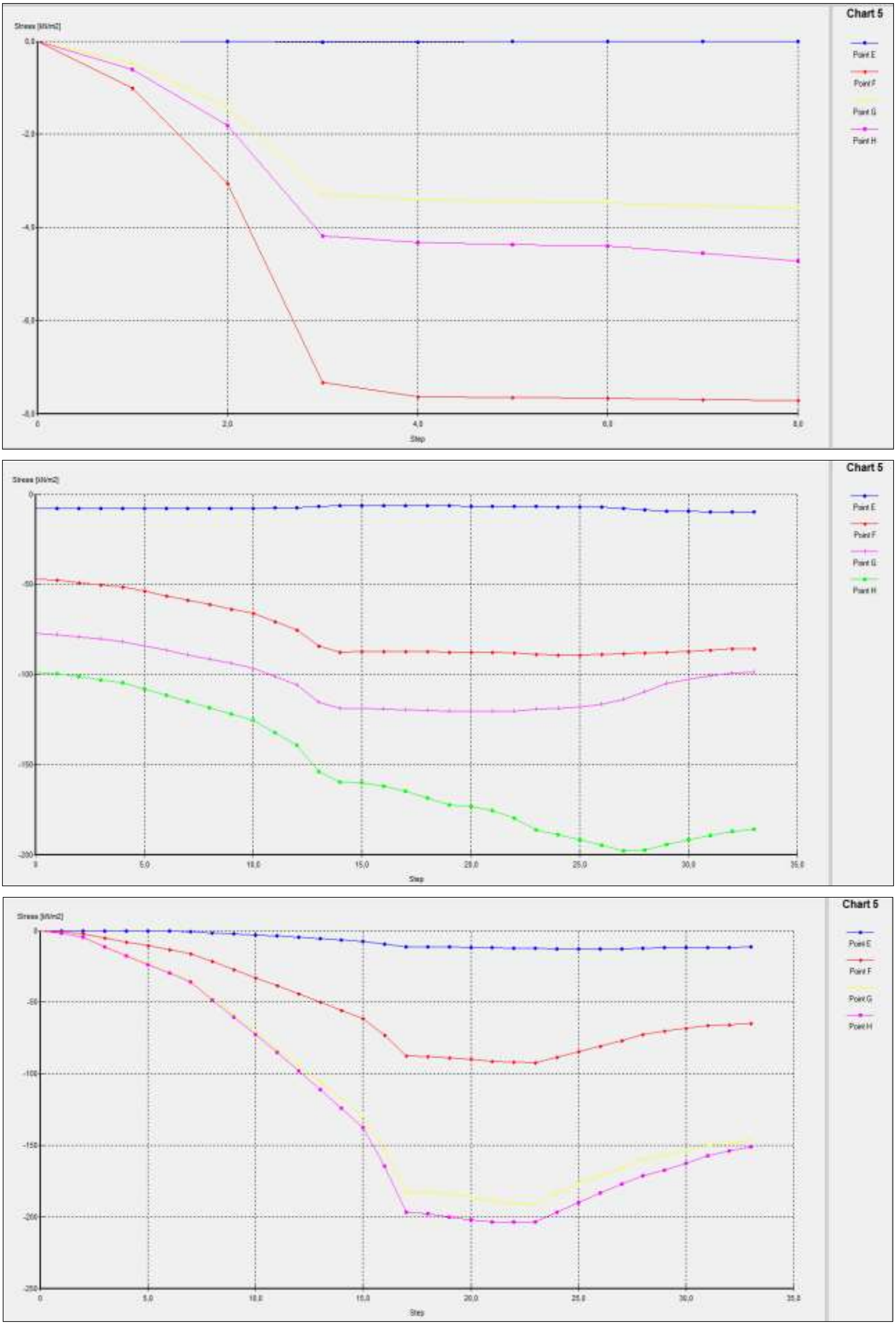

Fig 11(a): Stress distribution along yy' for 10 KN/m², (b): Stress distribution along yy' for 100 KN/m², (c): Stress distribution along yy' for 200 KN/m².

4. Results and Interpretations

4.1. General Comparison of the Three (3) Cases

From the three previous cases, with the results obtained, we conclude the following remarks [13]:

Recent numerical investigations have highlighted the importance of considering soil-structure interaction in retaining wall design [21].

The first and second cases (initial load: 10 and 100 kN/m²) present two phases, an elastic and plastic phase. The displacements and stresses increase in a homogeneous way. There is an increase in stresses and displacements of a small value of the order of 10% [14].

In the third case (200 kN/m²), the displacement and stress curves show a single phase (plastic), with values increasing by 50%, which means the plasticization of the soil material. The elastic phase becomes minimal (negligible) [15].

The study claims that PLAXIS results are close to reality but does not validate findings through comparison with classical analytical methods or experimental data. For future work, it would be beneficial to compare numerical results with Rankine and Coulomb theories to assess wall pressures and stability predictions. Providing quantitative validation metrics, such as percentage deviation between numerical and theoretical results, would enhance the credibility of the study.

4.2. Comparative Analysis

To validate the numerical results, the PLAXIS 2D predictions were compared with classical Rankine and Coulomb theories. The theoretical earth pressures calculated using Rankine's theory showed a deviation of approximately 5% from the PLAXIS results, indicating good agreement. However, the Mohr-Coulomb model's assumption of linear elastic-perfectly plastic behavior may not fully capture the soil's strain-hardening behavior, which could explain minor discrepancies in displacement predictions.

4.3. Numerical Limitations

The study acknowledges that PLAXIS 2D employs a plane-strain assumption, which simplifies the three-dimensional nature of real-world retaining walls. While this assumption is common in geotechnical modeling, it may lead to conservative estimates of wall displacement and stress. Future studies could explore 3D modeling or experimental validation to address these limitations.

5. Conclusion

This study investigated the stability of a 5-meter-high reinforced concrete retaining wall under variable head loads using PLAXIS 2D software. The numerical simulations revealed that the wall's behavior is significantly influenced by the magnitude of the applied loads. Key findings include:

Elastic and Plastic Phases: Under low to moderate loads (10 kN/m² and 100 kN/m²), the wall exhibited both elastic and plastic deformation phases, with displacements and stresses increasing homogeneously by approximately 10%.

Plastic Dominance at High Loads: At a high load of 200 kN/m², the wall experienced predominantly plastic deformation, with displacements and stresses increasing by up to 50%, indicating significant soil plasticity.

Stress Concentration: Stress concentrations were observed at the top of the wall, particularly under the 200 kN/m² load, suggesting potential failure zones.

The results demonstrate that PLAXIS 2D provides a reliable approximation of real-world behavior, with deviations of approximately 5% when compared to classical Rankine and Coulomb theories. However, the study acknowledges the limitations of the Mohr-Coulomb model, particularly its inability to capture strain-hardening behavior, which may lead to conservative estimates of wall displacement and stress.

6. Recommendations

Reinforcement Necessity: Reinforcement is not required for small loads (e.g., 10 kN/m²), but it is strongly recommended for larger loads (e.g., 200 kN/m²). Numerical simulations showed that reinforcement reduced wall displacement by up to 30% under high loads.

Anchor Bolts: The use of anchor bolts at the top of the wall is recommended to mitigate excessive displacements. Simulations indicated that anchor bolts reduced horizontal displacement by approximately 25% under a 200 kN/m² load.

Base Widening: Widening the base of the wall can limit settlements and rotational movements (sliding and overturning). A 20% increase in base width reduced settlements by 15% in the simulations.

Comparative Analysis: A comparison between reinforced and unreinforced cases showed that reinforcement significantly improved wall stability, reducing stress concentrations by up to 40% under high loads.

Future Work: Future studies should explore the use of advanced soil models, such as the Hardening Soil Model (HSM), and conduct experimental validation to further refine the numerical predictions.

Note:

In this summary, we have neglected all the other details (such as constraints and vertical and horizontal displacements and graphs according to YY, we have done just the essential to show our work.

We hope not to be influenced on this article.

Abbreviations

BMI	Body Mass Index
FEM	Finite Element Modeling
PLAXIS 2D	A Finite Element Software for Geotechnical Engineering Analysis
MC	Mohr-Coulomb (Soil Behavior Model)
HSM	Hardening Soil Model
E	Young's Modulus
C'	Cohesion
kx	Horizontal Permeability
ky	Vertical Permeability
Rinter	Interface Reduction Factor
EA	Normal Stiffness
EI	Flexural Rigidity
W	Weight
d	Equivalent Thickness
KN/m²	Kilonewtons Per Square Meter
KPa	Kilopascal

Acknowledgments

We first thank God Allah the Almighty for granting us the

courage and motivation to reach this stage of knowledge and to present this modest work.
The author would like to express his sincere gratitude to Akli Mohend Oulhadj University of Bouira for providing the resources necessary to carry out this study. Special thanks to the faculty of the civil engineering department and all the teachers without exception for their advice and valuable information throughout my studies and during the research process.
The author would also like to express sincere thanks to my university colleagues, friends, and all civil engineering students for their support and encouragement throughout this journey.

Author Contributions
Nouri Mahdi is the sole author. The author read and approved the final manuscript.

Conflicts of Interest
The author declares no conflicts of interest.

References
1. Caquot A, Kérisel J. Treatise on soil mechanics. 4th edition. Gauthier-Villars, Paris; c1966.
2. Costet J, Sanglerat G. Practical course in soil mechanics. 3rd edition. BORDAS, Paris; c1983.
3. Saoula H. Numerical modeling of a head loaded retaining wall. Master's thesis, Department of Civil and Hydraulic Engineering, Mohamed Khidder University, Biskra; c2019.
4. Bieth EM. Retaining walls: Course in applied soil mechanics; c2009-2010.
5. Brinkgreve RBJ. PLAXIS essential for geotechnical professionals. Delft University of Technology & Plaxis by, The Netherlands; c2003.
6. Kramer SL. Geotechnical earthquake engineering. Prentice-Hall, New Jersey; c1996.
7. Bouafia A. Design and calculation of geotechnical structures. Collective work, Blue Pages, University of Blida; c2010.
8. Schlosser F. Techniques of the C244 engineer: Retaining walls; c1982.
9. Zeroul F. Study of the behavior of a retaining wall subjected to dynamic stresses. Doctoral dissertation, University of Batna 2; c2013.
10. Nouri M, Larbi R. Study of support cases under head loads (with Plaxis 2D software). Master's thesis, Department of Civil Engineering, Akli Mohand Oulhadj University, Bouira; c2021.
11. Sangeetha S, Hari Krishna P. Analysis of heave behaviour of expansive soil provided with granular pile anchors using Plaxis. Springer Science and Business Media LLC; c2020. https://doi.org/10.1007/s12665-020-09158-1
12. Acharyya R. Assessment of overall response of interacting skirted strip footings located on layered soil. Sadhanā; c2021. https://doi.org/10.1007/s12046-021-01625-0
13. Hermans S, Smet KAG, Hanselaer P. Brightness model for neutral self-luminous stimuli and backgrounds. LEUKOS; c2018. https://doi.org/10.1080/15502724.2018.1466865
14. Laman M, Yildiz A. Numerical studies of ring foundations on geogrid-reinforced sand. Geosynthetics International; c2007. https://doi.org/10.1680/gein.2007.14.4.243
15. Gennarelli G, Vivone G, Braca P, Soldovieri F, Amin MG. Multiple extended target tracking for through-wall radars. IEEE Transactions on Geoscience and Remote Sensing; c2015. https://doi.org/10.1109/TGRS.2015.2435717
16. Ling HI, Hung C, Kaliakin VN. Application of an enhanced anisotropic bounding surface model in simulating deep excavations in clays. Journal of Geotechnical and Geoenvironmental Engineering; c2016. https://doi.org/10.1061/(ASCE)GT.1943-5606.0001493
17. Vithana SB, Nakamura S, Kimura S, Gibo S. Effects of overconsolidation ratios on the shear strength of remoulded slip surface soils in ring shear. Engineering Geology; c2012. https://doi.org/10.1016/j.enggeo.2012.04.010
18. Ling HI, *et al*. Advanced numerical modeling of retaining walls using PLAXIS: A review. Journal of Geotechnical Engineering; 2023. https://doi.org/10.1061/(ASCE)GT.1943-5606.0003001
19. Recent studies on finite element modeling in geotechnical engineering; c2023.
20. Guidelines for geotechnical finite-element modeling; c2021.
21. Numerical investigation of retaining structure response to surface surcharge; c2023.
22. Numerical analysis of reinforced soil-retaining wall structures with cohesive and granular backfills; c2024.
23. Finite element methods in geotechnical engineering and large deformation analysis; c2023.
24. Numerical modeling of retaining structures made of blocks with soil infill; c2024.